Biogeosciences Discuss., 11, 3241–3269, 2014
www.biogeosciences-discuss.net/11/3241/2014/
doi:10.5194/bgd-11-3241-2014

Biogeosciences Discussions
Open Access

Temperature-dependence of planktonic metabolism in the Subtropical North Atlantic Ocean

L. S. García-Corral[1], E. Barber[1], A. Regaudie-de-Gioux[1,2], S. Sal[2], J. Holding[1], S. Agustí[1,3], N. Navarro[4], P. Serret[5], P. Mozetič[6], and C. M. Duarte[1,3]

[1]Department of Global Change Research. IMEDEA (CSIC-UIB) Instituto Mediterráneo de Estudios Avanzados, Miquel Marqués 21, 07190 Esporles, Spain
[2]Centro Oceanográfico de Gijón, Instituto Español de Oceanografia, Avenida Principe de Asturias, 70 bis, 33212 Gijón, Spain
[3]The UWA Oceans Institute and School of Plant Biology, University of Western Australia, 35 Stirling Highway, Crawley 6009, Australia
[4]Área de Biodiversidad y Conservación ESCET, Universidad Rey Juan Carlos, Tulipán s/n, Móstoles, 28933 Madrid, Spain
[5]Departamento de Ecología y Biología Animal, Universidad de Vigo, 36200, Spain
[6]National Institute of Biology, Marine Biology Station, Fornace 41, 6330 Piran, Slovenia

Received: 22 January 2014 – Accepted: 31 January 2014 – Published: 26 February 2014

Correspondence to: L. S. García-Corral (lgarcia@imedea.uib-csic.es)

Published by Copernicus Publications on behalf of the European Geosciences Union.

BGD
11, 3241–3269, 2014

Abstract

The temperature dependence of planktonic metabolism in the Subtropical North Atlantic Ocean was assessed on the basis of measurements of gross primary production (GPP), community respiration (CR) and net community production (NCP), as well as experimental assessments of the response of CR to temperature manipulations. Metabolic rates were measured at 68 stations along three consecutive longitudinal transects completed during the Malaspina 2010 Expedition, in three different seasons. Temperatures gradients were observed in depth and at basin and seasonal scale. The results showed seasonal variability in the metabolic rates, being the highest rates observed during the spring transect. The overall mean integrated GPP/CR ratio was of 1.39 ± 0.27 decreasing from winter to summer and the NCP for the Subtropical North Atlantic Ocean during this cruises, was net autotrophy (NCP > 0) in about two-thirds of the total sampled communities (68.2 %). Here, we reported the activation energies describing the temperature-dependence of planktonic community metabolism, which generally was higher for CR than for GPP in the Subtropical North Atlantic Ocean, as the metabolic theory of ecology predicts. Also, we performed an assessment of the activation energies describing the responses to in situ temperature at field ($E_{aCR} = 1.64 \pm 0.36$ eV) and those derive experimentally by temperature manipulations ($E_{aCR} = 1.45 \pm 0.6$ eV), which showed a great consistency.

1 Introduction

The metabolic balance of plankton communities is a fundamental property controlling the role of plankton communities in the ocean's carbon budget (Duarte et al., 2011, 2013). In particular, net community production (NCP), the difference between gross primary production (GPP) and community respiration (CR), determines whether plankton communities act as CO_2 sinks (autotrophic communities, NCP > 0) or CO_2 sources (heterotrophic communities, NCP < 0).

BGD
11, 3241–3269, 2014

Recent analyses have point at seawater temperature as a driver of plankton community metabolism (Regaudie-de-Gioux and Duarte, 2012), consistent with metabolic theory of ecology (MTE, Brown et al., 2004; Gillooly et al., 2001), which predicts that both GPP and CR should increase with increasing temperature. MTE also leads to the expectation that the activation energy (E_a) for respiration should be higher than for photosynthesis (Harris et al., 2006), as confirmed by observations (López-Urrutia et al., 2006; Regaudie-de-Gioux and Duarte, 2012). Hence, plankton respiration rates are expected to increase faster with ocean warming than production rates. Consequently ocean warming should lead to a weakening of the CO_2 uptake by ocean biota, and may lead to a possible positive feedback in the carbon global budget (Duarte et al., 2012, 2013).

Resolving the temperature dependence of planktonic community metabolism is fundamental to predict the future role of plankton in the carbon budget of a warmer ocean. However, research on ocean planktonic community metabolism is still limited spatially and temporally, with measurements focused on restricted areas as the NE Atlantic Ocean, the Eastern Arctic Ocean, the Southern Ocean and the Mediterranean Sea (Robinson and Williams, 2005; Regaudie-de-Gioux and Duarte, 2013). Even in the North Atlantic basin, the most intensively studied area of the world's ocean, there is a paucity of estimates of net community metabolism in the western basin.

The North Atlantic Ocean plays an important role as a sink of atmospheric CO_2 (Sabine et al., 2004). However, it has been warming since the 1950's and increasing its heat content above the mean ocean rate ($0.3\,W\,m^{-2}$), exceeding $8\,W\,m^{-2}$ in the midlatitudes of the northwestern basin (Levitus et al., 2000, 2005). In addition, the subtropical North Atlantic Ocean shows a strong longitudinal and latitudinal temperature gradient, increasing from northwest Africa to northeast America, mainly due to the Gulf Stream and North Atlantic Current influence (Marshall et al., 2001). This temperature gradient suggests that metabolic rates may vary spatially and that the current warming trend may affect differentially planktonic communities in the western and eastern basin of the North Atlantic Ocean, which experience different thermal regimes.

BGD
11, 3241–3269, 2014

Here we assess the seasonal and regional variability on plankton metabolic rates in the Subtropical North Atlantic Ocean. We do so on the basis of near-zonal cruises conducted along three seasons (winter, spring and summer) in 2011. We also assess the thermal control on plankton metabolic rates, based on the in situ incubations and experimental temperature manipulations to examine the temperature dependence of community respiration rates.

2 Materials and methods

2.1 Study area

The study was conducted in the framework of the Malaspina 2010 Expedition, a circumnavigation project, which included three zonal cruises along the Subtropical North Atlantic Ocean, encompassing a latitudinal range spanning from 12.4° N to 41.6° N and a large longitudinal variation from −79.2° E to −14.7° E (Fig. 1). The first cruise (Leg 1) was conducted on board Spanish R/V *Sarmiento de Gamboa* sailing from the Gran Canary Island (Spain) to Florida (USA) along the 24° N parallel between 28 January and 9 March 2011, during the winter season. The second one (Leg 2) was also conducted on board Spanish R/V *Sarmiento de Gamboa*, sailed from Santo Domingo (Dominican Republic) to Vigo (Spain) from 23 March to 8 April, during springtime of 2011. The third and last cruise (Leg 3) was carried out on board Spanish R/V *Hespérides* sailing from Cartagena de Indias (Colombia) to Cartagena (Spain) during the summer of 2011, between 20 June and 10 July.

The three cruises included stations within five of the different biogeochemical provinces described by Longhurst (Longhurst, 1998, 2007). Sampled stations were mostly concentrated in 3 provinces: the North Atlantic Subtropical Gyre Province East (NASE or NAST-E), including 4 stations of Leg 1, 3 in Leg 2 and 7 in Leg 3; the North Atlantic Subtropical Gyre Province West (NASW) with 6 stations in each of Legs 1 and 2 were; and the North Atlantic Tropical Gyre Province (NATR), with 24 stations in Leg

BGD
11, 3241–3269, 2014

1, 3 in Leg 2 and 8 stations in Leg 3. The data set included stations in the Caribbean Province (CARB), with 1 station of Leg 2 and 5 on Leg 2, and 1 station of the Leg 1 was sampled within the North West Coastal Atlantic Shelves Province (NWCS) (Table 3, Fig. 2)

2.2 Community metabolism

Metabolic rates of the planktonic communities were measured at 35, 13 and 20 stations in Legs 1, 2 and 3, respectively, yielding a total of 68 stations (Fig. 1). During the three cruises seawater was sampled at 3 different depths within the photic layer. Surface waters (4.54 ± 2.48 m) were sampled with a 30 L Niskin bottle (between 3 and 5 m) during Leg 3 and with a Rosette sampler system for Leg 1 and 2. The Deep Chlorophyll Maximum (DCM, 114.11 ±4.12 m) which receives, on average, 1 % of the incident irradiance and an intermediate depth (43.09 ± 2.55 m), between surface and DCM, receiving 20 % of the incident radiation on the surface. Both depths were sampled using a Rosette sampler system fitted with a calibrated Sea-Bird SBE 9 CTD and 12 L Niskin bottles.

All seawater samples were directly siphoned from Niskin bottles into calibrated 100 mL borosilicate glass narrow-mouth Winkler bottles using a silicon tube.

For each depth, seven replicates were fixed (biological activity immediately stopped), to provide the initial oxygen concentration. The two other sets of seven replicates, dark and transparent, were filled and incubated for 24 h. The surface communities were incubated on deck for 24 h in a large 2000 L tank with continuous circulation of surface seawater to maintain the temperature of the surface waters and natural solar radiation. Bottles were covered with neutral screens to reduce incident radiation by 20 %, in addition to the 8 % to 12 % reduction in photosynthetically active radiation transmittance by the bottles themselves. The light conditions experienced by the incubated communities mimic those in the upper layer of the ocean but represent only an approximation, in that changes in the light environment due to mixing were not reproduced. For intermediate and DCM depths the dark and transparent bottles were placed inside opaque PVC

BGD
11, 3241–3269, 2014

and transparent polycarbonate incubation cylinders, respectively. Transparent incubation tubes were fitted with a combination of neutral density (LEE 210) and blue (HT061 Mist, 62.4 % transmission) filters to simulate the irradiance levels experienced by the community at their original sampling depth. Incubations tubes were filled with surface seawater and connected to a closed circuit pump incubator with a temperature-control holding the temperature to ±0.5 °C of the temperature in situ, set according to the temperature profile retrieved from the CTD cast. At the end of the incubation period, light and dark bottles from each depth were fixed to determine final O_2 concentrations.

Planktonic metabolism was evaluated from changes in dissolved oxygen concentrations, which were determined by automated high-precision Winkler titration with a potentiometric end-point Metrohm 808 Titrando (Oudot et al., 1988). CR and NCP were calculated from changes in dissolved oxygen concentrations, before and after incubation of samples under "dark" and "light" conditions, respectively, and GPP was calculated as NCP + CR (Carrit and Carpenter, 1966).

Rates are expressed as mmol O_2 m^3 d^{-1} and specific metabolic rates as mmol O_2 mg Chl a^{-1} d^{-1}. Integrated metabolic rates were calculated by the trapezoid method, from the surface layer to the DCM (1 %PAR) and standard errors were calculated using error propagation.

Total concentration of chlorophyll *a*, for Legs 2 and 3 was determined fluorometrically, (following Yentsch and Menzel, 1963), by acetone extraction of chlorophyll *a* on the cells retained in GF/F filters after filtering 200–500 mL samples (Estrada, 2012, 399). Chlorophyll *a* for Leg 1 was estimated from calibrated CTD fluorescence data (R^2 = 0.92, $p < 0.001$).

2.3 Experimental assessment of the temperature-dependence of community respiration rates

During the Leg 2, we performed experimental temperature manipulations at each of the 13 sampled stations to test the response of planktonic CR rates to temperature increase. Seawater was sampled from 10 m above the DCM and incubated at differ-

BGD
11, 3241–3269, 2014

ent temperatures. At this depth (10 m above DCM) plankton communities receive more light than at the DCM (Teira et al., 2005), but with almost same physical and chemical conditions, so production and biomass are expected to be close to the highest values in the water column. The chlorophyll maximum is somewhat deeper than the depth of maximum photosynthetic rate and of the biomass maximum for photosynthetic cells. In the Atlantic Ocean the DCM is not generally a biomass maximum but the result of a decrease of the carbon to chl *a* ratio with depth (Marañón et al., 2000). Seawater was siphoned into dark 100 mL Winkler bottles and incubated into opaque PVC tubes to protect them from light. Seven initial replicates were used to determine the initial oxygen concentration and other set of seven replicates were incubated for each different temperature treatment. We mimicked four temperatures of the in situ profiles: (1) in situ temperature at 10 m above DCM depth (80.97 ± 5.78 m), (2) that corresponding to an intermediate depth (44.61 ± 2.53 m), (3) surface (5–6 m) temperature and 3 °C above surface temperature. The resulting range of the experimental temperatures for incubations varied between 3 and 7 °C across the experiments performed. Experimental bottles were incubated for 24 h as indicated above and the CR rates were determinate following the same methodology as outlined above.

The activation energy (E_a) was derived from the slope of the Arrhenius plot, which represents the natural logarithm of Chl *a*-standardised $CR_{Chl\,a}$ and $GPP_{Chl\,a}$ rates (mmol O_2 mg Chl a^{-1} d^{-1}) against the inverted water temperature ($1/kT$) with k, the Boltzmann's constant (8.617734×10^{-5} eV K^{-1}) and T, temperature in Kelvin degrees (°K), following Regaudie de Gioux and Duarte (2012). The Q_{10} value, which provides an estimate of the relative increase in metabolic rates expected for a 10 °C temperature increase, was calculated from the equation (Raven and Geider, 1988):

$$Q_{10} = e^{\left(\frac{10E_a}{RT^2}\right)} \quad (1)$$

where R is the gas constant (8.314472 mol^{-1} K^{-1}), and T is the mean absolute temperature across the range over which Q_{10} was measured (K) and E_a is the activation energy (J mol^{-1}).

BGD
11, 3241–3269, 2014

2.4 Satellite images

Satellite images were retrieved from the AQUA MODIS (or Moderate Resolution Imaging Spectroradiometer) satellite. In order to make a unique map for each cruise, images of chlorophyll *a* and surface water temperature were created using an average of 8 days, from the central day-station of the cruise (i.e: Leg 1: central date was 19 February 2011 and the average image was from 18 February 2011 to 25 February 2011). The information was processed with the SeaDAS software and maps were created using ArcGis software by Esri.

3 Results

The three cruises were characterized by a gradient from cooler waters in the eastern basin to warmer waters in the western basin (Fig. 2). Seasonal temperature differences were also significant with mean temperature (±SE) of $22.4 \pm 0.13\,^{\circ}C$ for Leg 1, during the Northern Hemisphere winter, $19.5 \pm 0.62\,^{\circ}C$ for Leg 2 during spring, but at higher latitudes, and warmer temperatures, with a mean temperature of $24.4 \pm 0.45\,^{\circ}C$ during Leg 3 in summer. The seawater temperature also declined by about $1.7\,^{\circ}C$ (Leg 1), $1.1\,^{\circ}C$ (Leg 2) and $3.7\,^{\circ}C$ (Leg 3) from the surface to the DCM depth (Table 1, Fig. 2). The deep chlorophyll maximum depth (Z_{DCM}), varied greatly between a minimum of 20 m in Leg 2 and a maximum of 165 m in Leg 1, with a mean value of 114.11 ± 4.12 m for all stations and (mean ± SE) 119.03 ± 4.84 m, 90.95 ± 12.96 m and 120.55 ± 6.26 m for Leg 1, 2 and 3 respectively (Table 2, Fig. 2).

Chlorophyll *a* concentrations showed significant variations, temporally and spatially. The mean chlorophyll *a* concentration showed a similar same range for Leg 1 (0.20 ± 0.01 mg Chl $a\,m^{-3}$) and Leg 3 (0.21 ± 0.02 mg Chl $a\,m^{-3}$) (*t* test, $p > 0.05$), but both differed significantly from the mean chlorophyll *a* concentration during Leg 2 ($0.30 \pm 0.07\,mg\,m^{-3}$) (*t* test $p < 0.005$). This difference is due to the maximum value of chlorophyll *a* measured at the Eastern basin during Leg 2 in surface waters (1.63 mg

BGD
11, 3241–3269, 2014

Chl $a\,m^{-3}$, Table 1, Fig. 2). The satellite imagery revealed a region of high chlorophyll *a* concentrations in the Eastern basin, affected by the Northwest African upwelling (Fig. 3). Most of the stations were occupied within the highly oligotrophic waters of the Subtropical Gyre, except for the northern stations in the eastern basin during Leg 2, which extended to more productive waters (Figs. 2 and 3). Chlorophyll a concentrations decreased significantly with seawater temperature ($R^2 = 0.26$, $p < 0.0001$, $N = 192$) and increased with depth from surface waters to DCM depths in Legs 1 and 3. In Leg 2, higher chlorophyll *a* concentrations were found in surface and 20 % PAR depths than at the DCM (Table 1, Fig. 2), which represented therefore a fluorescence, but not chlorophyll maximum.

The overall mean of volumetric GPP rate for the study area was $1.42 \pm 0.16\,mmol\,O_2\,m^{-3}\,d^{-1}$. GPP varied from below detection limit during the winter and summer cruises respectively at superficial waters to a maximum value of $18.01 \pm 0.11\,mmol\,O_2\,m^{-3}\,d^{-1}$ at the hottest Caribbean waters (36.64 m, 28.72 °C) during Leg 3. The highest GPP rates were measured at the surface during Leg 1 but at the intermediate depth (20 %PAR) during Leg 2 and 3. The highest mean of GPP rates were registered during Leg 2 ($2.59 \pm 0.43\,mmol\,O_2\,m^{-3}\,d^{-1}$), indicating a GPP significantly higher in spring than in summer or winter (*t* test, $p < 0.0001$) (Table 1).

The overall mean of volumetric CR rate for the study area was $1.70 \pm 0.23\,mmol\,O_2\,m^{-3}\,d^{-1}$. Volumetric CR rates followed similar patterns as GPP, with a minimum of $0.01 \pm 0.27\,mmol\,O_2\,m^{-3}\,d^{-1}$ during Leg 1 (103 m, 21.5 °C) and $0.01 \pm 0.15\,mmol\,O_2\,m^{-3}\,d^{-1}$ during Leg 3 (100 m, 18.21 °C) at deep and cold waters and a maximum of $28.42 \pm 0.11\,mmol\,O_2\,m^{-3}\,d^{-1}$ during Leg 3 at the Caribbean hot waters (23.49 m, 28.39 °C). Volumetric CR rates were significantly lower during Leg 1 (on average, $1.10 \pm 0.12\,mmol\,O_2\,m^{-3}\,d^{-1}$) than during Leg 2 (on average, $2.33 \pm 0.32\,mmol\,O_2\,m^{-3}\,d^{-1}$) and Leg 3 (on average, $2.29 \pm 0.77\,mmol\,O_2\,m^{-3}\,d^{-1}$) (*t* test $p < 0.0001$, Table 1), with this two last transects showing similar mean values.

The overall mean NCP rate was positive, indicative of a global autotrophic planktonic metabolism across Legs ($0.19 \pm 0.24\,mmol\,O_2\,m^{-3}\,d^{-1}$), with higher rates observed at

BGD
11, 3241–3269, 2014

the 20 % PAR depth (Table 1). NCP showed no significant differences between cruises (t test, $p = 0.84$), but showed contrasting vertical patterns in each Leg. The communities sampled along Leg 1 were net autotrophic (NCP = 0) from surface to DCM. During Leg 2, autotrophic communities prevailed in the surface layers and heterotrophic communities dominated deeper depths, while Leg 3 showed the reverse pattern, with heterotrophic and autotrophic communities prevailing in surface layers and deeper layers, respectively (Table 1).

The integrated GPP rates were about 135.14 ± 21.76, 134.70 ± 20.50 and 64.02 ± 5.07 mmol O_2 m^{-2} d^{-1} for Legs 1, 2 and 3 respectively. The minimum and maximum integrated GPP were observed in Leg 1 (28.65 ± 45.55 and 411.8 ± 86.05 mmol O_2 m^{-2} d^{-1}) in the western and eastern basin respectively. Integrated CR showed also a minimum and maximum in Leg 1 (6.45 ± 44.1 and 494.85 ± 34.17 mmol O_2 m^{-2} d^{-1}). The highest mean integrated CR (± SE) rate was observed in Leg 2 (182.10 ± 43.47 mmol O_2 m^{-2} d^{-1}) and similar CR integrated rates were observed for Leg 1 (146 ± 21.76 mmol O_2 m^{-2} d^{-1}) and Leg 3 (142.02 ± 44.65 mmol O_2 m^{-2} d^{-1}) (Table 2).

Integrated NCP rates varied greatly from net autotrophic (NCP > 0) to net heterotrophic (NCP < 0) across stations and Legs. However, the medians of integrated NCP showed a prevalence of autotrophic communities (median NCP = 36.00 ± 29.44, 21.30 ± 37.95 and 61.20 ± 53.97 mmol O_2 m^{-2} d^{-1} for Legs 1, 2 and 3, respectively) (Table 2). The mean integrated GPP/CR ratio confirmed an overall net autotrophic metabolism, with an overall mean of 1.39 ± 0.27 and no significant difference between Legs (ANOVA, $p > 0.05$). However, it is observed that the median GPP/CR ratio decreased from Leg 1 to Leg 3 (Tables 1 and 2). Using integrated rates, autotrophic communities (NCP > 0) represented about two-thirds of the total sampled stations (70.59 %, 61.54 % and 68.42 % for Legs 1, 2 and 3, respectively).

Net autotrophic communities were dominant across the 5 different Longhurst biogeochemical provinces (Longhurst, 1998, 2007) occupied during the three Legs (Table 3). Mean NCP rates showed no significant differences between provinces, being the NASE

BGD
11, 3241–3269, 2014

province the most autotrophic region. Mean CR showed significant differences between provinces, but only due to extreme heterotrophic community sampled at 23.24 m in the coastal Caribbean area. The mean GPP decreased from the most productive province, the NASE through the CARB, NASW, NWCS and being the NATR the most oligotrophic region. The mean GPP/CR ratio showed no significant differences between provinces and all showed medians were above 1 (Table 3).

$CR_{Chl\ a}$ and $GPP_{Chl\ a}$ rates, binned by 1 °C, showed an increased with increasing seawater temperature for Leg 2 (linear regression, $R^2 = 0.50$, $p = 0.01$; $R^2 = 0.60$, $p = 0.005$, respectively), while in Leg 1, $CR_{Chl\ a}$ showed a significant temperature-dependence (linear regression, $R^2 = 0.62$, $p = 0.036$) but not $GPP_{Chl\ a}$ (linear regression, $R^2 = 0.32$, $p > 0.05$). In Leg 3, $GPP_{Chl\ a}$ increased with temperature (linear regression, $R^2 = 0.36$, $p = 0.05$) but there was no significant relation for $CR_{Chl\ a}$ (linear regression, $R^2 = 0.13$, $p > 0.05$) (Fig. 4). The activation energies (E_a) and corresponding Q_{10} values for $CR_{Chl\ a}$ were higher than those for $GPP_{Chl\ a}$ in Leg 1 and 2, but not in Leg 3 (Table 4). The experimental temperature manipulations showed a significant increase of $CR_{Chl\ a}$ with increasing temperature ($R^2 = 0.65$, $p = 0.0009$). The E_a derived from the experiments of temperature-dependence of $CR_{Chl\ a}$ (1.64 ± 0.36 eV) was not significantly different from those derived from in situ data (Table 4, Fig. 5), demonstrating consistency between experimental and in situ relationships. Indeed, use of the Arrhenius linear relationship derived experimentally from temperature manipulations to predict the in situ values yields predicted values consistent with the observed ones, with the slope of the relationship between observed and predicted $CR_{Chl\ a}$ not differing significantly from 1 (linear regression model II equation, slope (±SE) = 1.32 ± 0.23).

4 Discussion

Plankton metabolism showed considerable variation along the longitudinal sections examined in this study of the Subtropical North Atlantic Ocean. Plankton metabolism

BGD
11, 3241–3269, 2014

had been poorly studied in the Western basin of the North Atlantic Ocean, as almost all rates reported for the Northern Subtropical Atlantic derived from Eastern basin (Reguadie-de-Gioux and Duarte, 2012), except a few studies derived from the Bermuda Atlantic Time-series Study (BATS) in the Sargasso Sea (Williams et al., 2013). Indeed, Western and Eastern basin, separated by the Mid-Atlantic Ridge, differ significantly in key physical, chemical and biological properties, such as water temperature, chlorophyll *a* concentrations and salinity (Sathyendranath et al., 1995; Li and Harrison, 2001). Our results show a longitudinal Eastward decrease temperature gradient from warmer superficial waters at the Western basin to a cooler Eastern basin, with colder areas supporting higher chlorophyll *a* concentrations. The lowest chlorophyll- a concentrations were found in the oligotrophic Subtropical North Atlantic Gyre region, and the highest rates corresponded to waters of the northwest African upwelling (González et al., 2002). The chlorophyll a concentration values were on average (0.22 ± 0.02 mg Chl $a\,m^{-3}$) within the ranges previously reported for the North and South Atlantic Subtropical Gyres (González et al., 2002; Teira et al., 2005). Mean surface chlorophyll *a* concentration (0.16 ± 0.02 mg Chl $a\,m^{-3}$) for the three cruises was higher than the 0.09 ± 0.01 mg Chl $a\,m^{-3}$ reported by Teira et al. (2005) for the Eastern basin of the Subtropical North Atlantic. The integrated chlorophyll *a* concentration (21.73 ± 0.35 mg chl $a\,m^{-2}$) is representative of oligotrophic waters ranging from 20 to 40 mg Chl $a\,m^{-2}$ (Marañón et al., 2000).

Here we report a high temporal and spatial variability of the metabolic rates in the Subtropical North Atlantic Ocean, which can be due to seasonal forcing affecting temperature and nutrient supply and physical mechanisms that alter the water column structure (Gruber et al., 2002), such as mesoscale instabilities (González et al., 2001; Garçon et al., 2001), and intrinsic factors, such as changes in community structure (Serret et al., 2009) in response to physical forcing. High temporal and spatial variability of metabolic rates between stations and cruises has been observed in the Subtropical North Atlantic Ocean, with higher GPP and CR rates in spring time, (González et al., 2002) and in the eastern basin, while lower metabolic rates were found in winter and

BGD
11, 3241–3269, 2014

summer time and in the West basin. During the spring season in the mid-latitude North Atlantic Ocean, the westerly winds decrease and the solar radiation increase, supporting the conditions for a phytoplankton bloom (Harrison et al., 2001). Depletion of nutrients with higher stratification of the water column in summer leads to a decrease in productivity and metabolic rates (González et al., 2001), with a secondary bloom developing with the onset of mixing during fall and a subsequent decrease of photosynthetic rates with the reduction of solar radiation during winter (Longhurst, 1998).

Whereas previous results have suggested a prevalence of heterotrophic metabolism in the Subtropical North Atlantic Gyre (Duarte et al., 2001), the Subtropical North Atlantic Ocean showed a net metabolic balance in this study, with a prevalence of autotrophy (68.2 % of the communities). Heterotrophic metabolism has been argued to prevail in oligotrophic gyres (del Giorgio et al., 1997; Duarte and Agusti, 1998; Duarte et al., 2013), consistent with an abundance of reports of net heterotrophic metabolism in plankton communities of the Subtropical North Atlantic (Duarte et al., 2001; González et al., 2002; Serret et al., 2002, 2006; Morán et al., 2004; Aranguren-Gassis et al., 2011). However, some studies have also shown balanced metabolism (Williams, 1998; Aranguren-Gassis and Serret, 2012) or even a prevalence of autotrophic communities (Kähler et al., 2010), leading to challenges in the view that oligotrophic regions of the ocean support heterotrophic plankton communities (Williams et al., 2013). The eastern basin of the North Atlantic receives allochthonous organic carbon inputs, both as production exported from the North African upwelling (Pelegrí et al., 2005) and atmospheric inputs (Dachs et al., 2005), which must, therefore, support balanced or autotrophic metabolism, whereas such sources of allochthonous organic carbon and nutrients are less evident in the Western basin.

The metabolic theory of ecology (MTE, Gillooly et al., 2001; Brown et al., 2004) predicts an increase in the metabolic rates with increasing temperature, confirmed for plankton communities (López-Urrutia et al., 2006; Regaudie-de-Gioux and Duarte, 2012). Our results confirm these expectations and show a clearly temperature-dependence of standardized chlorophyll *a* metabolic rates (GPP and CR) along the

BGD
11, 3241–3269, 2014

temperature range measured (14 to 29 °C). The activation energy values for GPP and CR were 2 to 4.5-fold higher than those reported by Regaudie-de Gioux and Duarte, 2012, (E_{aGPP} = 0.32 eV and E_{aCR} = 0.66 eV), measured across a much wider temperature range (0 to 29 °C) across the ocean. The empirical activation energies for CR reported in this study showed consistently steeper values than those derived by López-Urrutia et al. (2006) (E_{aCR} = 0.65 eV) and Regaudie-de-Gioux and Duarte (2012) for Atlantic communities (E_{aCR} = 0.92 eV), those inferred from ETS activity (Arístegui and Montero,1995; E_{aCR} = 0.70 eV) and that observed for respiration rates in aquatic ecosystems in general (Yvon-Durocher et al., 2012; E_{aCR} = 0.65 eV). The results presented here also confirm a general higher activation energy for CR than GPP in the Subtropical North Atlantic Ocean, consistent with expectations from Metabolic Theory (Brown et al., 2004; Harris et al., 2006; López-Urrutia et al., 2006) and previous global analyses (Regaudie-de Gioux and Duarte, 2012). However, the experimental E_{aCR}, at 1.64 ± 0.36 eV, was higher, although not significantly so, than the average (1.45 ± 0.6 eV) determined through comparative analyses across communities, suggested that the temperature-dependence of plankton communities exposed to short-term temperature increase overestimates that of communities pre-adapted to different temperature regimes. Most importantly, our results show a remarkable consistency between activation energies for respiration rate derived from the comparative analysis of in situ rates, and that derived from experimental manipulation of temperature. Hence, the temperature-dependence of planktonic metabolism reported here helps explaining spatial and seasonal patterns in planktonic metabolism in the open ocean. Our results showed the high vulnerability of the Subtropical North Atlantic Ocean to a sea water temperature increase, fact to be under consideration, due to the forecasted ocean warming between 1–3 °C by the end of the century predicted in the last IPCC (2007) report. North Atlantic Ocean constitutes the largest ocean sink for atmospheric CO_2in the Northern Hemisphere (Gruber et al., 2002) and long-term trends indicates that the subtropical gyre of theNorth Atlantic is at present acting as a significant and detectable sink for anthropogenic CO_2 (Bates et al., 2002).

BGD
11, 3241–3269, 2014

This consistency confirms the predictive power of the metabolic theory of ecology to predict the responses of plankton community metabolism to foretell negative feedbacks of warming on the CO_2 sink capacity of marine biota (López-Urrutia et al., 2006), possibly shifting communities (Lomas and Bates, 2004) toward a higher prevalence of heterotrophy across the Subtropical North Atlantic.

Acknowledgements. This is a contribution to the Malaspina Expedition 2010, funded by the INGENIO 2010 CONSOLIDER program (ref. CDS2008-00077) of the Spanish Ministry of Economy and Competitiveness. We thank the captains and crews of R/V *Sarmiento de Gamboa* and R/V *Hespérides* and the UTM for the their help onboard and technical support, M. Fuster for help with mapping and satellite imagery, and the participants of the Malaspina Expedition and Buque Escuela projects for providing CTD data and general support. L. S. García-Corral was supported by a JAE Pre-doc fellowship, from the Spanish National Research Council (CSIC) and the BBVA Foundation, Spain.

References

Aranguren-Gassis, M. and Serret, P.: Balanced plankton net community metabolism in the oligotrophic North Atlantic subtropical gyre from Lagrangian observations, Deep-Sea Res. Pt. I, 68, 116–122, 2012.

Aranguren-Gassis, M., Serret, P., Fernández, E., Herrera, J. L., Domínguez, J. F., Pérez, V., and Escanez, J.: Production and respiration control the marine microbial metabolic balance in the eastern North Atlantic subtropical gyre, Deep-Sea Res. Pt. I, 58, 768–775, 2011.

Arístegui, J. and Montero, M. F.: The relationship between community respiration and ETS activity in the ocean, J. Plankton Res., 17, 1563–1571, 1995.

Bates, N. R., Pequignet, A. C., Johnson, R. J., and Gruber, N.: A short-term sink for atmospheric CO_2 in subtropical mode water of the North Atlantic Ocean, Nature, 420, 489–493, 2002.

Brown, J. H., Gillooly, J. F., Allen, A. P., Savage, V. M., and West, G. B.: Toward a metabolic theory of ecology, Ecology, 85, 1771–1789, 2004.

Carritt, D. E. and Carpenter, J.: Comparison and evaluation of currently employed modifications of winkler method for determining dissolved oxygen in seawater – a Nasco report, J. Mar. Res., 24, 286–318, 1966.

BGD
11, 3241–3269, 2014

Dachs, J., Calleja, M. L., Duarte, C. M., Del Vento, S., Turpin, B., Polidori, A., and Agustí, S.: High atmosphereocean exchange of organic carbon in the NE subtropical Atlantic. Geophys. Res. Lett., 32,L21807, 2005.

Del Giorgio, P. A., Cole, J. J., and Cimbleris, A.: Respiration rates in bacteria exceed phytoplankton production in unproductive aquatic systems, Letters to Nature, 385, 1997.

Duarte, C. M. and Agusti, S.: The CO_2 balance of unproductive aquatic ecosystems, Science, 281, 234–236, 1998.

Duarte, C. M., Agustí, S., Arístegui, J., González, N., and Anadón, R.: Evidence for a heterotrophic subtropical northeast Atlantic, Limnol. Oceanogr., 46, 425–428, 2001.

Duarte, C. M., Agustí, S., and Regaudie-de-Gioux, A.: 2011. The role of marine biota in the metabolism of the biosphere,p. 39–53. In: Duarte, C. M., [ed.], The role of marine biota in the functioning of the biosphere. Fundación BBVA, Bilbao.

Duarte, C. M., Agustí, S., Wassmann, P., Arrieta, J. M., Alcaraz, M., Coello, A., Marbà, N., Hendriks, I. E., Holding, J., García-Zarandona, I., Kritzberg., E. and Vaqué, D.: Tipping elements in the Arctic marine ecosystem, Ambio, 41, 44–55, 2012.

Duarte, C. M., Regaudie-de-Gioux, A., Arrieta, J. M., Delgado-Huertas, A., and Agustí, S.: The oligotrophic ocean is heterotrophic, Annu. Rev. Mar. Sci., 5, 551–569, 2013.

Estrada, M.: Determinación fluorimétrica de la concentración de clorofila *a*, in: Expedición de Circunnavegación Malaspina 2010, Cambio Global y Exploración de la Biodiversidad del Océano, edited by: Moreno-Ostos, E., Libro Blanco de Métodos y Técnicas de Trabajo Oceanográfico, CSIC, Madrid, 399–406, 2012.

Garçon, V. C., Oschlies, A., Doney, S. C., McGillicuddy, D., and Waniek, J.: The role of mesoscale variability on plankton dynamics in the North Atlantic, Deep-Sea Res. Pt. II, 48, 2199–2226, 2001.

Gillooly, J. F., Brown, J. H., West, G. B., Savage, V. M., and Charnov, E. L.: Effects of size and temperature on metabolic rate, Science, 293, 2248–51, 2001.

González, N., Anadón, R., Mouriño, B., Fernández, E., Sinha, B., Escánez, J., and De Armas, D.: The metabolic balance of the planktonic community in the North Atlantic Subtropical Gyre: the role of mesoscale instabilities, Limnol. Oceanogr., 46, 946–952, 2001.

González, N., Anadón, R., and Marañón, E.: Large-scale variability of planktonic net community metabolism in the Atlantic Ocean: importance of temporal changes in oligotrophic subtropical waters, Mar. Ecol. Prog. Ser., 233, 21–30, 2002.

BGD
11, 3241–3269, 2014

Gruber, N., Keeling, C. D., and Bates, N. R.: Interannual variability in the North Atlantic Ocean carbon sink, Science, 298,5602, 2374–8, 2002.
Harris, L. A., Duarte, C. M., and Nixon, S. W.: Allometric laws and prediction in estuarine and coastal ecology, Estuar. Coast., 29, 340–344, 2006.
Harrison, W., Aristegui, J., Head, E. J., Li, W. K., Longhurst, A., and Sameoto, D.: Basin-scale variability in plankton biomass and community metabolism in the sub-tropical North Atlantic Ocean, Deep-Sea Res. Pt. II, 48, 2241–2269, 2001.
IPCC 2007 Climate change 2007: the physical sciences basis. In Contribution of Working Group I to the fourth assessment report of the Intergovernmental Panel on Climate Change. (eds M. L. Parry, O. F. Canziani, J. P. Palutikof, P. J. van der Linden and C. E. Hanson), pp. 7–22. Cambridge, UK: Cambridge University Press.
Kähler, P., Oschlies, A., Dietze, H., and Koeve, W.: Oxygen, carbon, and nutrients in the oligotrophic eastern subtropical North Atlantic, Biogeosciences, 7, 1143–1156, doi:10.5194/bg-7-1143-2010, 2010.
Levitus, S., Antonov, J. I., Boyer, T. P., and Stephens, C.: Warming of the World Ocean, Science, 287, 2225–2229, 2000.
Levitus, S., Antonov, J., and Boyer, T.: Warming of the world ocean,1955–2003. Geophys. Res. Lett., 32, L02604, 2, 2005.
Li, W. K. and Harrison, W.: Chlorophyll, bacteria and picophytoplankton in ecological provinces of the North Atlantic, Deep-Sea Res. Pt. II, 48, 2271–2293, 2001.
Lomas, M. W. and Bates, N. R.: Potential controls on interannual partitioning of organic carbon during the winter/spring phytoplankton bloom at the Bermuda Atlantic Time-series Study (BATS) site, Deep-Sea Res. Pt. I, 51, 1619–1636, 2004.
Longhurst, A.: Ecological Geography of the Sea, Academic Press, San Diego, CA, 1998.
Longhurst, A.: Ecological Geography of the Sea, 2nd ed., Academic Press, San Diego, CA, 2007.
López-Urrutia, A., San Martin, E., Harris, R. P., and Irigoien, X.: Scaling the metabolic balance of the oceans, P. Natl. Acad. Sci. USA, 103, 8739–8744, 2006.
Marañón, E., Holligan, P. M., Varela, M., Mouriño, B., and Bale, A. J.: Basin-scale variability of phytoplankton biomass, production and growth in the Atlantic Ocean, Deep-Sea Res. Pt. I, 47, 825–857, 2000.

BGD
11, 3241–3269, 2014

Marshall, J., Kushnir, Y., Battisti, D., Chang, P., Czaja, A., Dickson, R., and Visbeck, M.: North Atlantic climate variability: phenomena, impacts and mechanisms, Int. J. Climatol., 21, 1863–1898, 2001.

Morán, X., Fernández, E., and Pérez, V.: Size-fractionated primary production, bacterial production and net community production in subtropical and tropical domains of the oligotrophic NE Atlantic in autumn, Mar. Ecol.-Prog. Ser., 274, 17–29, 2004.

Oudot, C., Gerard, R., Morin, P., and Gningue, I.: Precise shipboard determination of dissolved-oxygen (Winkler Procedure) for productivity studies with a commercial system, Limnol. Oceanogr., 33, 146–150, 1988.

Pelegrí, J. L., Arístegui, J., Cana, L., González-Dávila, M., Hernández-Guerra, A., Hernández-León, S., and Santana-Casiano, M.: Coupling between the open ocean and the coastal upwelling region off northwest Africa: water recirculation and offshore pumping of organic matter, J. Marine Syst., 54, 3–37, 2005.

Raven, J. A. and Geider, R. J.: Temperature and algal growth, New Phytol., 110, 441–461, 1988.

Regaudie-de-Gioux, A. and Duarte, C. M.: Temperature dependence of planktonic metabolism in the ocean, Global Biogeochem. Cy., 26, 1–10, 2012.

Regaudie-de-Gioux, A. and Duarte, C. M.: Global patterns in oceanic planktonic metabolism, Limnol. Oceanogr., 58, 977–986, 2013.

Robinson, C. and le B. Williams, P. J.: Respiration and its measurement in surface marine waters, in: Respiration in Aquatic Ecosystems, edited by: del Giorgio, P. and le B. Williams, P. J., Oxford Univ. Press, Cambridge, UK, 148–181, 2005.

Sabine, C. L., Feely, R. A., Gruber, N., Key, R. M., Lee, K., Bullister, J. L., and Rios, A. F.: The oceanic sink for anthropogenic CO_2, Science, 305, 367–371, 2004.

Sathyendranath, S., Longhurst, A., Caverhill, C. M., and Platt, T.: Regionally and seasonally differentiated primary production in the North Atlantic, Deep-Sea Res. Pt. I, 42, 1773–1802, 1995.

Serret, P., Fernández, E., and Robinson, C.: Biogeographic differences in the net ecosystem metabolism of the open ocean, Ecology, 83, 3225–3234, 2002.

Serret, P., Fernandez, E., Robinson, C., Woodward, E. M. S., and Perez, V.: Local production does not control the balance between plankton photosynthesis and respiration in the open Atlantic Ocean, Deep-Sea Res. Pt. I, 53, 1611–1628, 2006.

BGD
11, 3241–3269, 2014

Serret, P., Robinson, C., Fernández, E., Teira, E., Tilstone, G., and Pérez, V.: Predicting plankton net community production in the Atlantic Ocean, Deep-Sea Res. Pt. II, 56, 941–953, 2009.

Teira, E., Mourino, B., Maranon, E., Perez, V., Pazo, M., Serret, P., Dearmas, D., Escanez, J., Woodward, E., and Fernandez, E.: Variability of chlorophyll and primary production in the Eastern North Atlantic Subtropical Gyre: potential factors affecting phytoplankton activity, Deep-Sea Res. Pt. I, 52, 569–588, 2005.

le B Williams, P. J., Quay, P. D., Westberry, T. K., and Behrenfeld, M. J.: The oligotrophic ocean is autotrophic, Annu. Rev. Mar. Sci., 5, 535–549, 2013.

le B Williams, P. J.: The balance of plankton respiration and photosynthesis in the open oceans, Nature, 394, 55–57, 1998.

Yentsch, C. S. and Menzel, D. W.: A method for determination of chlorophyll and phaeophytin by fluorescence, Deep-Sea Res. Pt. I, 10, 221–231, 1963.

Yvon-Durocher, G., Caffrey, J. M., Cescatti, A., Dossena, M., Giorgio, P. Del, Gasol, J. M., Montoya, J. M., Pumpanen, J., Staehr, P. a, Trimmer, M., Woodward, G. and Allen, A. P.: Reconciling the temperature dependence of respiration across timescales and ecosystem types., Nature, 487, 472–476, 2012.

BGD
11, 3241–3269, 2014

Table 1. Mean (±SE) temperature (°C), chlorophyll *a* (mg Chl *a* m^{-3}), and volumetric metabolic rates (GPP, CR and NCP) for the three depths sampled in Leg 1, 2 and 3 and GPP/CR ratio.

		LEG 1 (Jan–Mar) 2012			LEG 2 (Mar–Apr) 2012			LEG 3 (Jun–Jul) 2012		
		Surface	20 %PAR	DCM	Surface	20 %PAR	DCM	Surface	20 %PAR	DCM
Temperature (°C)	Mean ± SE	23 ± 0.17	22.93 ± 0.17	21.29 ± 0.21	19.9 ± 1.15	19.71 ± 1.12	18.77 ± 0.99	25.83 ± 0.64	25.2 ± 0.7	22.38 ± 0.66
	Range	20.59–24.84	20.59–24.79	19.34–24.28	14.74–25.41	14.75–25.68	14.31–24.81	20.93–29.10	20.83–29.11	17.43–27.42
	N	35	32	34	13	13	12	20	19	19
	Mean Leg ± E		22.42 ± 0.13			19.48 ± 0.62			24.49 ± 0.42	
Chlorophyll *a* ($mg\,m^{-3}$)	Mean ± SE	0.13 ± 0.01	0.15 ± 0.01	0.3 ± 0.02	0.35 ± 0.14	0.31 ± 0.12	0.25 ± 0.10	0.1 ± 0.02	0.09 ± 0.01	0.43 ± 0.03
	Range	0.08–0.23	0.10–0.25	0.14–0.51	0.02–1.63	0.03–1.56	0.03–1.32	0.04–0.31	0.05–0.21	0.22–0.77
	N	35	32	34	11	12	12	20	20	20
	Mean Leg ± SE		0.2 ± 0.01			0.30 ± 0.07			0.21 ± 0.02	
GPP ($mmol\,O_2\,m^{-3}\,d^{-1}$)	Mean ± SE	1.08 ± 0.24	1.39 ± 0.27	0.96 ± 0.11	3.34 ± 0.75	3.5 ± 0.92	0.94 ± 0.16	0.62 ± 0.08	1.87 ± 1.08	0.46 ± 0.06
	Range	0.00–6.52	0.04–6.08	0.01–2.34	0.65–10.71	0.22–11.42	0.09–2.13	0.00–1.60	0.23–18.01	0.13–0.87
	N	33	27	26	13	11	12	18	16	12
	Mean Leg ± SE		1.14 ± 0.12			2.59 ± 0.43			1.01 ± 0.38	
CR ($mmol\,O_2\,m^{-3}\,d^{-1}$)	Mean ± SE	1.05 ± 0.20	1.15 ± 0.23	1.11 ± 0.20	2.49 ± 0.51	2.54 ± 0.65	1.96 ± 0.52	0.98 ± 0.19	3.91 ± 1.95	2.12 ± 1.31
	Range	0.04–4.61	0.03–4.40	0.01–4.79	0.35–7.20	0.46–8.17	0.38–7.21	0.09–3.07	0.19–28.42	0.01–16.25
	N	33	27	26	13	12	12	18	16	12
	Mean Leg ± SE		1.10 ± 0.12			2.33 ± 0.32			2.29 ± 0.77	
NCP ($mmol\,O_2\,m^{-3}\,d^{-1}$)	Mean ± SE	0.28 ± 0.29	0.53 ± 0.27	0.23 ± 0.24	0.85 ± 0.66	0.62 ± 0.85	−0.88 ± 0.52	−0.1 ± 0.25	−1.08 ± 1.43	0.92 ± 1.64
	Range	−3.77–4.85	−2.88–5.66	−4.14–4.68	−3.40–6.83	−4.65–7.86	−6.63–0.67	−2.85–2.89	−27.27–4.22	−16.12–27.20
	N	35	32	34	13	13	13	20	20	20
	Mean Leg ± SE		0.34 ± 0.15			0.20 ± 0.4			−0.09 ± 0.72	
GPP/CR	Mean ± SE		3.77 ± 0.88			1.31 ± 0.16			1.23 ± 0.19	
	Range		0.00–57.00			0.07–3.74			0.00–6.42	
	N		86			36			45	
	Median		1.32			1.06			0.96	

BGD
11, 3241–3269, 2014

Table 2. Mean (±SE), range, number of observations (*N*) and median for the integrated metabolic rates (GPP, CR and NCP), GPP/CR ratio and the depth at which the DCM was located for Legs 1, 2 and 3.

		LEG 1 (Jan–Mar) 2012	LEG 2 (Mar–Apr) 2012	LEG 3 (Jun–Jul) 2012
INTEGRATED GPP (mmol O_2 m^{-2} d^{-1})	Mean ± SE	135.14 ± 21.76	134.7 ± 20.50	64.02 ± 5.07
	Range	28.65–411.80	58.00–259.39	46.08–84.97
	N	22	11	9
	Median	98.5	124.10	69.35
INTEGRATED CR (mmol O_2 m^{-2} d^{-1})	Mean ± SE	146.98 ± 25.68	182.1 ± 43.47	142.02 ± 44.65
	Range	6.45–494.85	29.31–473.81	27.23–447.08
	N	21	12	9
	Median	131.73	133.70	83.16
INTEGRATED NCP (mmol O_2 m^{-2} d^{-1})	Mean ± SE	42.97 ± 29.44	-50.28 ± 37.95	73.56 ± 53.97
	Range	-426.70–743.40	-332.20–76.00	-401.00–733.20
	N	34	13	19
	Median	36.00	21.30	61.20
GPP/CR	Mean ± SE	1.74 ± 0.51	1.18 ± 0.20	0.84 ± 0.20
	Range	0.14–11.13	0.27–2.35	0.10–1.74
	N	21	11	9
	Median	1.16	1.17	0.77
Z_{DCM} (m)	Mean ± SE	119.03 ± 4.84	90.95 ± 12.96	120.55 ± 6.26
	Range	35.00–165.00	20.00–156.00	71.05–161.26
	N	35	13	20
	Mean Z_{DCM} ± SE		114.11 ± 4.12	

BGD
11, 3241–3269, 2014

Table 3. Mean (±SE), range, number of observations (*N*) and median of metabolic rates (GPP, CR, NCP) and GPP/CR ratio for the Longhurst biogeochemical provinces crossed in the study area.

		GPP (mmol O_2 m^{-3} d^{-1})	CR (mmol O_2 m^{-3} d^{-1})	NCP (mmol O_2 m^{-3} d^{-1})	GPP/CR
NASE	Mean ± SE	2.28 ± 0.52	1.70 ± 0.21	0.79 ± 0.37	3.08 ± 1.69
	Range	0.00–11.42	0.01–3.88	−3.23–7.86	00.00–55.00
	N	32	32	38	32
	Median	0.78	1.31	0.25	1.18
NATR	Mean ± SE	0.92 ± 0.09	1.38 ± 0.22	0.02 ± 0.23	3.35 ± 0.88
	Range	0.00–3.69	0.01–16.25	−16.12–5.66	00.00–57.00
	N	85	86	102	85
	Median	0.72	0.81	0.08	0.99
NASW	Mean ± SE	1.53 ± 0.21	1.60 ± 0.34	0.00 ± 0.27	2.16 ± 0.41
	Range	0.02–5.35	0.06–8.17	−6.63–2.76	0.02–10.17
	N	35	35	39	35
	Median	1	0.92	0.31	1.33
NWCS	Mean ± SE	1.21 ± 0.21	0.87 ± 0.22	0.34 ± 0.02	1.49 ± 0.19
	Range	0.81–1.51	0.43–1.17	0.31–0.38	1.29–1.88
	N	3	3	3	3
	Median	1.31	1	0.34	1.31
CARB	Mean ± SE	2.27 ± 1.31	4.27 ± 2.40	0.22 ± 2.20	1.35 ± 0.24
	Range	0.26–18.01	0.09–28.42	−27.27–27.20	0.04–2.89
	N	13	13	18	13
	Median	1.00	1.04	0.22	1.12

BGD
11, 3241–3269, 2014

Table 4. Q_{10}, activation energy (eV) as the slope of the regression and the parameters of the Arrhenius relationship between the natural logarithm of chlorophyll *a*-specific metabolic rates (mmol O_2 mg Chl a^{-1} d^{-1}) binned by 1 °C and inverted temperature ($1/kT$) for each Leg (1, 2 and 3) and the temperature manipulation experiments in Leg 2.

	Temperature Range	Rate	Intercept ± SE	Slope ± SE	R^2	p	n	Q_{10}
Leg 1	19.3–24.8 °C	GPP	29.94 ± 18.17	−0.72 ± 0.46	0.32	0.18	7	2.60
		CR	55.73 ± 18.9	−1.37 ± 0.48	0.62	0.036*	7	6.17
Leg 2	14.3–25.7 °C	GPP	58.52 ± 15.16	−1.41 ± 0.38	0.60	0.005*	11	6.77
		CR	72.16 ± 23.31	−1.74 ± 0.59	0.50	0.01*	11	10.59
Leg 3	17–29 °C	GPP	58.12 ± 25.10	−1.44 ± 0.64	0.36	0.05*	11	6.61
		CR	50.52 ± 28.89	−1.23 ± 0.74	0.13	0.23	11	5.02
Experimental Temperature Manipulation	14–30 °C	CR	67.60 ± 14.43	−1.64 ± 0.36	0.65	0.0009*	13	9.11

BGD
11, 3241–3269, 2014

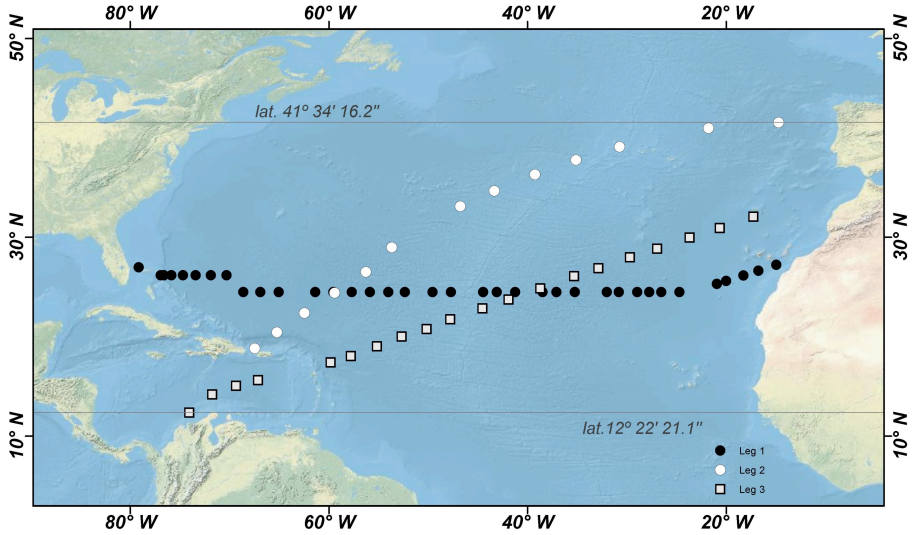

Fig. 1. Map showing the stations occupied on Leg 1 (full circles), Leg 2 (open circles) and Leg 3 (open squares) during the Malaspina 2010 Expedition.

BGD
11, 3241–3269, 2014

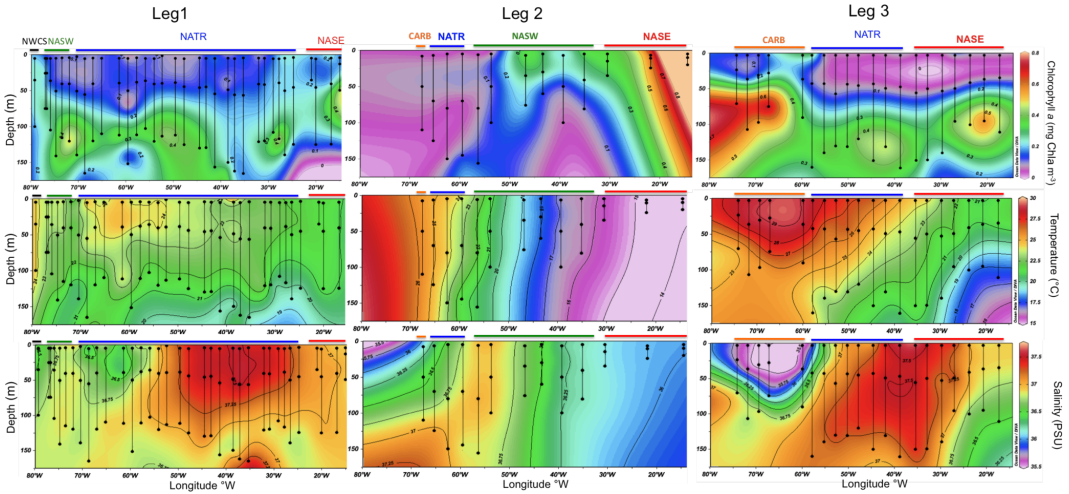

Fig. 2. Contour plots for chrolophyll *a* (mg Chl *a* m^{-3}), temperature (°C) and salinity of the profiles sampled in (left) Leg 1, (middle) Leg 2, (right) Leg 3.

BGD
11, 3241–3269, 2014

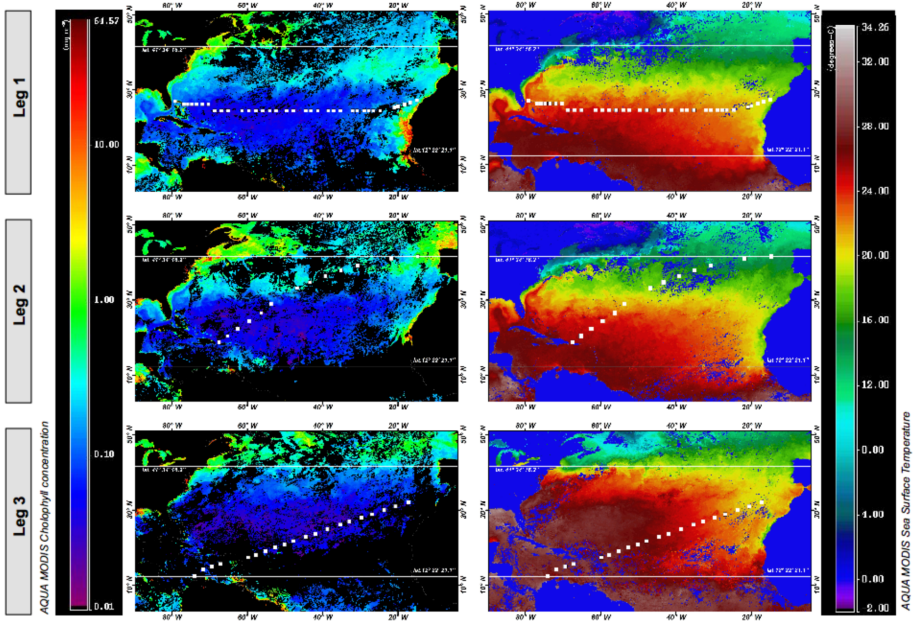

Fig. 3. Satellite images showing 8 day-average chlorophyll *a* and surface water temperature from the date of the central station sampled in Legs 1, 2 and 3.

BGD
11, 3241–3269, 2014

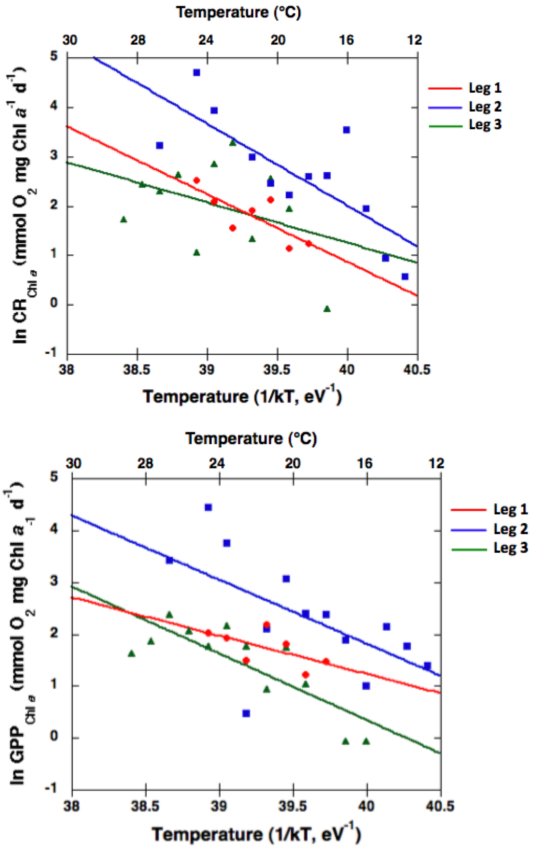

Fig. 4. Arrhenius plots showing the relationship between chl *a*-specific average rates ($GPP_{Chl\,a}$ and $CR_{Chl\,a}$) within 1 °C bins and the inverted water temperature ($1/kT$, where k is the Boltzmann's constant, 8.629 10^{-5} eVk^{-1}, and T is the water temperature in °K) for Legs 1, 2 and 3.

BGD
11, 3241–3269, 2014

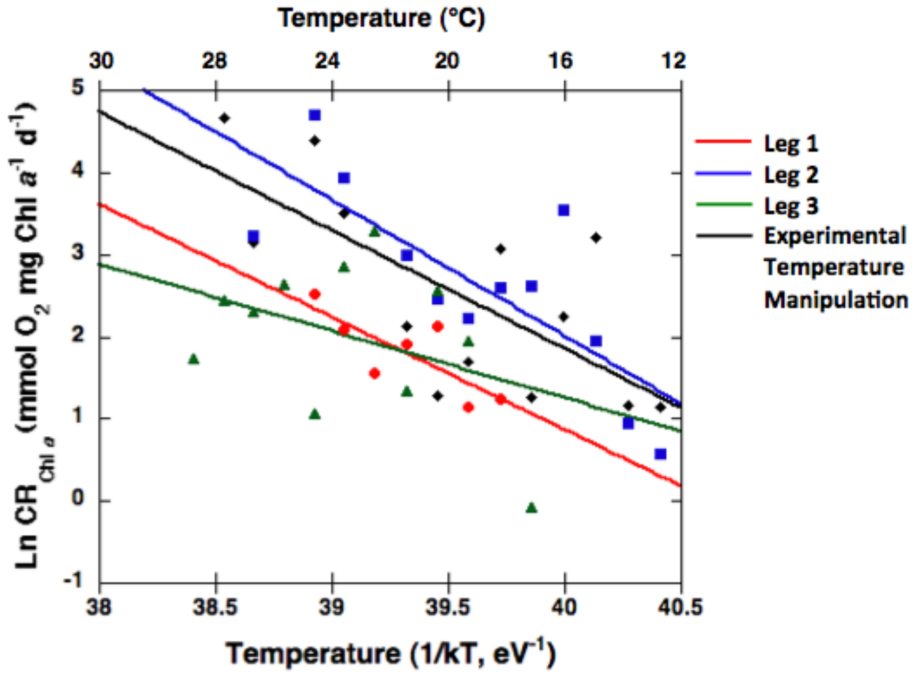

Fig. 5. Arrhenius plot showing the relationship between average chl a-specific respiration rate within 1 °C bins and the inverted water temperature ($1/kT$, where k is the Boltzmann's constant, 8.629×10^{-5} eV k^{-1}, and T is the water temperature in °K) for experimental temperature manipulations conducted during Leg 2 as well Arrhenius plots for Legs 1, 2 and 3 for comparison.

BGD
11, 3241–3269, 2014